Pressure Control Mechanism and Heat Transfer Characteristics of Hybrid Control Rod for Passive IN-core Cooling System in SMR

Kyung Mo Kim, In Cheol Bang *
Department of Nuclear Engineering
Ulsan National Institute of Science and Technology (UNIST)
50 UNIST-gil, Ulju-gun, Ulsan, 44919, Republic of Korea
Corresponding author: icbang@unist.ac.kr

1. Introduction

For the high levels of safety and reliability of the nuclear power plants, various types of small modular reactors (SMRs) are under development worldwide. The advantages of SMRs (long-term operation, economic, and safety) are attained because most of them are integral reactors, which contain the primary, secondary, and passive safety systems within a reactor pressure vessel; therefore, the loss of coolant accident, which is a representative postulated accident in commercial nuclear reactors, can be prevented. However, the dependence of the passive safety systems causes high uncertainty in operation during accident conditions due to lack of research for thermal-hydraulic phenomena in passive safety systems and lack of operation experience. Installation of additional passive safety system which operates with different working principle compared to existing systems can mitigate and solve the problems related to the uncertainty by providing the diversity of the safety systems. The application of hybrid control rod to SMRs can be a candidate for additional passive decay heat removal systems. The hybrid control rod is a device that combines the functions of control rod (reactor shutdown by neutron absorption) and heat pipe (heat transfer between hotter and colder section by phase change and convection of working fluid in closed metal container). Thus, the replacement of existing control rods to hybrid control rods can provide a direct way for decay heat removal from the core to additional heat sink. Maximum heat removal capacity of the hybrid control rod is determined by flooding phenomena which is caused by countercurrent flow between vapor and liquid. The operation limit of the heat pipe increases with the operating pressure as presented in many previous studies [1-5]. Thus, the hybrid control rod must operate at high operating pressure (> 15 bar) to achieve the significant decay heat removal capacity [6]. The strategy for controlling operating pressure inside the hybrid control rod was established to use the volume expansion of the working fluid and charge of non-condensable gas without installation of any pressure control devices. Hence, the thermal performances, variation of operating pressure, and operation limits of the hybrid control rod according to amounts of working fluid and non-condensable gas were experimentally studied in this paper. The measured operation limits of the hybrid control rod in various conditions were compared with the values predicted by previously developed model.

2. Experiment

In this section, experimental setup including the test section which is scaled-down hybrid control rod is introduced. The experimental procedures to measure the thermal performances and operation limits of the hybrid control rods are mentioned.

2.1 Test Section

The composition of the experimentally studied test section is shown in Fig. 1. A 1-m-long stainless steel 316L test section with 25.4 mm outer diameter and 22 mm inner diameter was used as a cladding which contains the working fluid and neutron absorber. The neutron absorber material (B_4C) pellet with outer diameter and length of 17.7 mm and 285 mm, respectively, was contained in the evaporator section. The working fluid (deionized water) was charged to the test section with various fill ratios (fraction of volumes between working fluid and evaporator section).

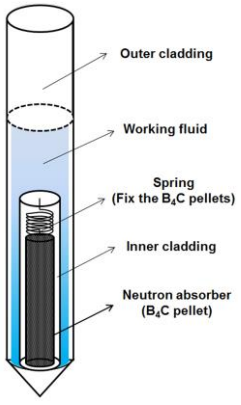

Fig. 1. Drawing of composition of hybrid control rod.

2.2 Experimental Setup and Procedures

The test facility comprises as shown in Fig. 2; a test section, a water jacket which takes a role of condenser to condense the evaporated working fluid, and a pump that circulates coolant from the water storage tank to

the water jacket. The evaporator section of the hybrid control rod was heated by Joule heating method with the copper electrodes connected to DC power supply. Sixteen K-type thermocouples (TCs) were installed on wall of the test section (six on the evaporator, six on the adiabatic, and four on condenser sections). The temperatures at the inlet and outlet of water jacket were also measured to quantify the heat removal rate through the water jacket. The internal pressure of the test section was measured by pressure transducer installed on the top of the test section. The experimental procedure is as follows; the working fluid was charged into test section, then the nitrogen gas was injected to the test section for the initial pressurization. After preparing the test section to targeted initial conditions, coolant was circulated through water jacket with a constant flow rate and loads the heat in the evaporator section.

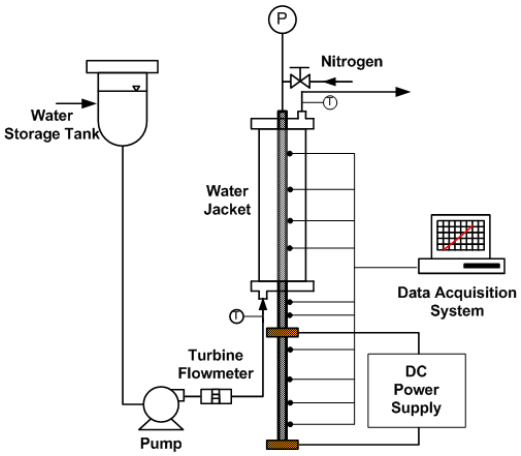

Fig. 2. Schematic diagram of hybrid control rod test facility.

2.3 Test Matrix

The operating pressure of the hybrid control rod must be controlled without any control devices to attain the passive operation concept. The use of volume expansion of the working fluid and charge of the non-condensable gas inside the hybrid control rod was selected as a strategy for the pressure control.

Table I: Experimental conditions

Parameter	Values
Heat load [W]	400 – 5200
Coolant flow rate [kg/s]	0.025
Fill ratio [%]	200 – 350 (90 – 130 mL)
Initial pressure [bar]	1.0 – 7.0 bar

According to amounts of charged working fluid, the pressurization rate and thermal performances can be varied. The charge of the non-condensable gas can extend the limited operating pressure of the hybrid control rod formed by volume expansion to the higher levels. Thus, the effects of initial charges of working fluid and non-condensable on the thermal performances and pressurization of the test section were studied with the test matrix presented in Table 1.

3. Results and Discussion

The wall temperatures and internal pressure were recorded during the experiments. Based on the measured parameters, the pressurization, thermal performances, and operation limits were deduced.

3.1 Variation of Operating Pressure

Effect of fill ratio of the working fluid on the pressurization of the test section was investigated as shown in Fig. 3. The initial pressure of the test section was atmospheric pressure.

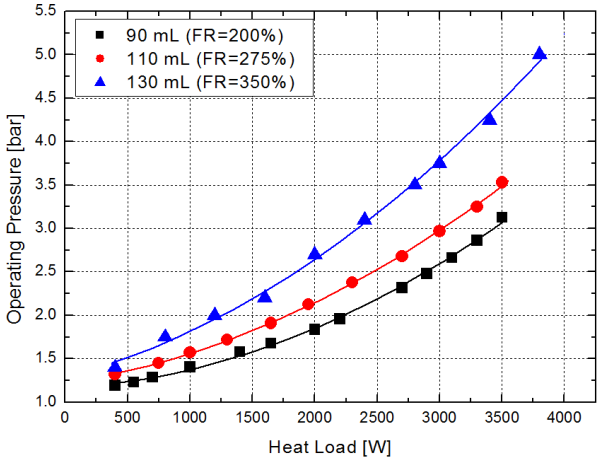

Fig. 3. Variations of operating pressures according to fill ratios of working fluid and heat loads.

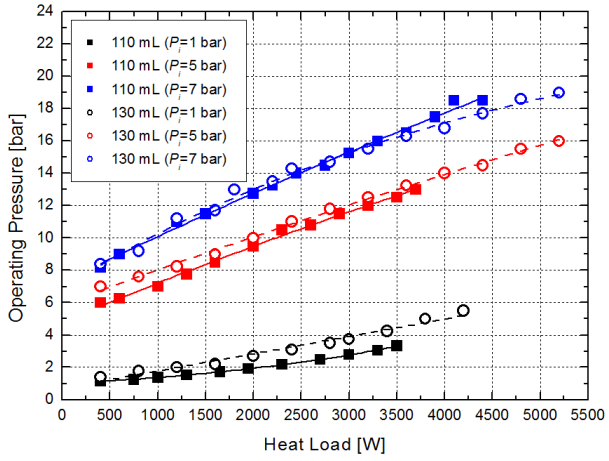

Fig. 4. Variations of operating pressures according to fill ratios of working fluid, initial pressures, and heat loads.

The operating pressure increased with the heat loads. The pressurization rate was increased as the amount of

working fluid increases. Maximum operating pressure was 5.0 bar for 130 mL (FR=350%), however; that is insufficient to achieve the target value (higher than 15.0 bar). Hence, non-condensable gas was initially charged to enhance the operating pressure of the hybrid control rod in the working fluid of 110 and 130 mL-charged conditions. The variations of operating pressures for nitrogen-charged test sections are shown in Fig. 4. The pressurization rates of the test sections become similar as the initial pressure increases as can be seen in the slope of the pressure according to heat loads. As the initial pressure of the test section increases, the effect of the fill ratio on the pressurization decreased because the amount of nitrogen gas charged in the test section increases with the initial pressure and dominates the internal pressure. In the test sections with initial pressure of 7 bar, the targeted operating pressures (> 15 bar) were achieved without relevant to fill ratio of the working fluid.

3.2 Evaporation Heat Transfer

The heat transfer coefficients of the test sections were calculated using the wall temperature distributions at each steady state. The evaporation heat transfer coefficients of the test sections for various fill ratios with initial pressure of 1 bar is shown in Fig. 5.

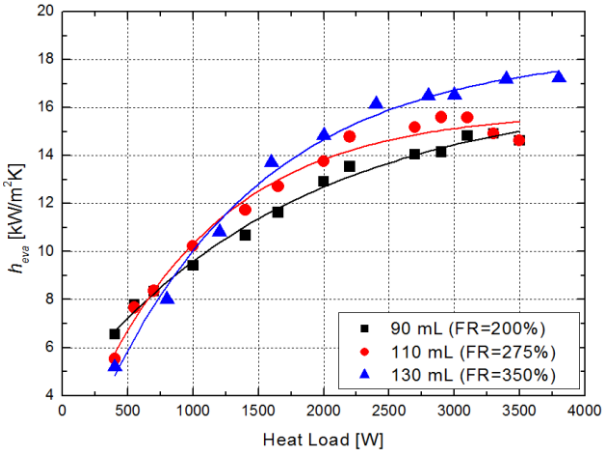

Fig. 5. Evaporation heat transfer coefficients according to fill ratios of test sections with 1 bar initial pressure.

The enhanced heat transfer coefficients were observed as the amount of the working fluid increases. The enhancement of the heat transfer coefficients is related to the variation of the internal pressure of the test section according to heat loads. The increase in the amount of working fluid causes the higher pressurization rate. As the internal pressure increases, the latent heat will be reduced resulting in the acceleration of the phase change. Hence, the evaporator heat transfer was enhanced as the fill ratio increases. The evaporation heat transfer coefficients of the conditions of initial pressures and fill ratios are shown in Fig. 6.

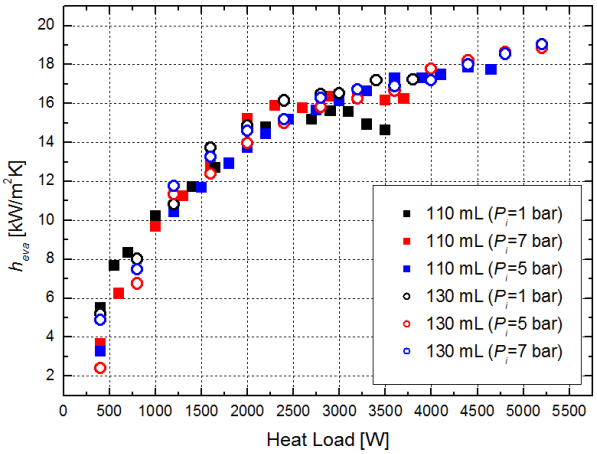

Fig. 6. Evaporation heat transfer coefficients according to fill ratios and initial pressures of test sections.

There are no definite relationship between heat transfer coefficients and initial pressures, and fill ratios of the working fluid. In the atmospheric pressure, the amount of the working fluid affected the heat transfer characteristics in terms of thermodynamics. However, the nitrogen-charged test sections showed similar pressurization rates because nitrogen gas dominates the change in internal pressures. Thus, the effect of initial pressures and fill ratios of the working fluid on the evaporation heat transfer was negligible in the presence of non-condensable gas conditions as presented in previous study [7].

3.3 Operation Limit

The maximum heat removal capacities of the hybrid control rods were compared with those predicted by existing correlations which were modeled to analyze the flooding limit of the thermosyphon as shown in Fig. 7.

$$Q_{\text{Imura}} = 0.64\rho_v H_{lv} A\left(\frac{D}{4L}\right)\left(\frac{\rho_l}{\rho_v}\right)^{0.13}\sqrt[4]{\sigma g\left(\rho_l-\rho_v\right)/\rho_v^2} \quad (1)$$

$$Q_{\text{ESDU}} = f_1 f_2 f_3 A_{cs} h_{lv}\rho_v^{1/2}\left[\sigma g\left(\rho_l-\rho_v\right)\right]^{1/4} \quad (2)$$

$$Q_{\text{Wallis}} = C_w^2 h_{lv} A\rho_v^{1/2}\left[gD\left(\rho_l-\rho_v\right)\right]^{1/2}\left[1+m\left(\frac{\rho_v}{\rho_l}\right)^{1/4}\right]^{-2} \quad (3)$$

$$Q_{\text{Faghri}} = Kh_{lv} A_v\left[g\sigma\left(\rho_l-\rho_v\right)\right]^{1/4}\left[\rho_v^{-1/4}+\rho_l^{-1/4}\right]^{-2} \quad (4)$$

$$Q_{\text{Tien and Chung}} = C_k^2 h_{lv} A_v\left[g\sigma\left(\rho_l-\rho_v\right)\right]^{1/4}\left[\rho_v^{-1/4}+\rho_l^{-1/4}\right]^{-2} \quad (5)$$

The operation limits were proportional to the fill ratio of the working fluid and operating pressures [7]. In low operating pressure region (< 10 bar), Wallis

model showed good agreement with the experimentally measured operation limits. The ESDU correlation predicted the operation limits of the hybrid control rods well in high operating pressures (> 10 bar). However, the tendency about the amounts of working fluid and non-condensable gas is unclear because the existing correlations do not consider the effect of the fill ratios and non-condensable gas. Therefore, new model considering the effect of fill ratios and non-condensable gas on the operation limit will be developed by further studies.

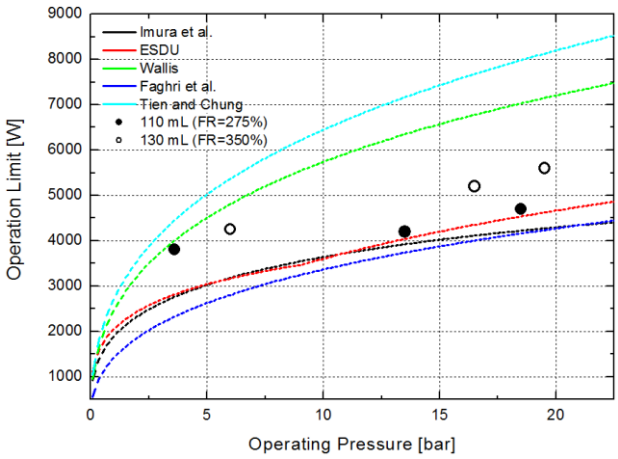

Fig. 7. Comparison of operating limits between existing correlations and experimentally measured values.

4. Conclusions

For the development of hybrid control rod which operates at high saturation pressures by self-pressurization process, the thermal performances of the hybrid control rods with various amounts of working fluid and non-condensable gas were experimentally studied. Following results were obtained:

(1) The pressurization rate and maximum operating pressure were increased as the amount of working fluid in the test section increases, however; the effect of fill ratio was decreased as the amount of non-condensable gas increases.
(2) Evaporation heat transfer coefficients increase with the fill ratio of the working fluid due to higher pressurization rate followed by the acceleration of the phase change.
(3) In high pressure ranges, the non-condensable gas dominates the internal pressure of the test section resulting in the similar heat transfer coefficients among the various test conditions.
(4) Maximum heat removal capacity of the hybrid control rod was proportional to operating pressure and fill ratio of the working fluid.
(5) Several correlations predicting the operation limit of the thermosyphon showed good agreement with the measured values according to saturation pressure ranges, however; new model considering the effect of non-condensable gas and fill ratio on the operation limit must be developed.

ACKNOWLEDGEMENTS

This work was supported by the Nuclear Energy Research Program through the National Research Foundation of Korea (NRF) funded by the Ministry of Science, ICT, and Future Planning. (No. NRF-22A20153413555)

REFERENCES

[1] H. Imura, K. Sasaguchi, H. Kozai, Critical Heat Flux in a Closed Two-phase Thermosyphon, International Journal of Heat and Mass Transfer, Vol.26, p. 1181, 1983.
[2] Engineering Science Data Unit, heat pipes-Performance of two-phase closed thermosyphons, Data item No. 81038, ESDU, London, 1981.
[3] G. Wallis, One-dimensional two-phase flow, McGraw-Hill, New York, 1969.
[4] A. Faghri, M. M. Chen, M. Morgan, Heat Transfer Characteristics in Two-phase Closed Conventional and Concentric Annular Thermosyphons, Journal of Heat Transfer, Vol.111, p. 611, 1989.
[5] C. L. Tien, K. S. Chung, Entrainment Limits in Heat Pipes, AIAA Journal, Vol. 17, p. 643, 1978.
[6] Y. S. Jeong, K. M. Kim, I. G. Kim, I. C. Bang, Hybrid Heat Pipe based passive In-core Cooling System for Advanced Nuclear Power Plant, Applied Thermal Engineering, Vol. 90, p. 609, 2015.
[7] K. M. Kim, I. C. Bang, Comparison of Flooding Limit and Thermal Performance of Annular and Concentric Thermosyphons at Different Fill Ratios, Applied Thermal Engineering, Vol. 99, p. 179, 1999.